Experimental Thermal and Fluid Science 60 (2015) 201–207

Contents lists available at ScienceDirect

Experimental Thermal and Fluid Science

journal homepage: www.elsevier.com/locate/etfs

Generation mechanism of micro-bubbles in a pressurized dissolution method

Yasunari Maeda [a], Shigeo Hosokawa [a,*], Yuji Baba [a], Akio Tomiyama [a], Yoshihiro Ito [b]

[a] Department of Mechanical Engineering, Graduate School of Engineering, Kobe University, 1-1 Rokkodai, Nada, Kobe 657-8501, Japan
[b] Housing Systems Business Group, Panasonic Corporation, 1048 Kadoma, Osaka 571-8686, Japan

ARTICLE INFO

Article history:
Received 4 June 2014
Received in revised form 18 September 2014
Accepted 18 September 2014
Available online 26 September 2014

Keywords:
Micro-bubble
Pressurized dissolution method
Cavitation
Bubble diameter
Bubble number density
Multiphase flow

ABSTRACT

Micro-bubbles are in use in many industrial fields such as water treatment, purification of lake water, chemical engineering, washing processes and housing equipment by virtues of their large interfacial area concentration and long residence time in liquid. A pressurized dissolution method based on decompression of liquid with dissolved gas is one of promising methods for generating fine micro-bubbles at high number density. Since the mechanism of micro-bubble generation is not clarified yet, design and improvement of micro-bubble generators are based on trial and error. In this study, effects of liquid volume flux at a decompression nozzle and dissolved gas concentration in the upstream region of the nozzle on diameter and number density of generated micro-bubbles are examined to understand generation mechanism of micro-bubbles in a pressurized dissolution method. The diameter and the number density of micro-bubbles are measured by using phase Doppler anemometry (PDA) in the downstream region of the nozzle, and the flow patterns in the nozzle are visualized by using a high-speed camera. The experimental results show that diameter and number density of generated micro-bubbles depend on cavitation pattern at the nozzle, and that cavitation bubbles containing not only vapor but also non-condensable gas become micro-bubbles due to their shrink caused by condensation of the vapor in the downstream region of the nozzle.

1. Introduction

Micro-bubbles are the bubbles with diameter ranging from one to several hundred microns, and they are characterized by a large interfacial area concentration per unit gas volume and low relative velocity between the bubbles and liquid phase. These characteristics are of great use in enhancement of adsorption of impurities at gas–liquid interface and mass transfer between the two phases [1,2]. Micro-bubbles are, therefore, utilized to improve efficiencies and/or performances of various industrial systems such as chemical reactors [3], water treatment systems [4], washing processes [5], medical systems [6], bathing systems [7] and plant cultivation [8]. Since efficiencies and performances of these systems depend on the diameter and number density of micro-bubbles, it is important to optimize them in development of the micro-bubble generators [9,10] and to understand a mechanism of micro-bubble generation.

Various types of micro-bubble generators have been developed, and most of them can be classified into four methods, i.e., the method based on bubble breakup due to shear flow/pressure wave (bubble breakup method [11,12]), the method using ultrasonic wave (ultrasonic method [13,14]), the method using microfluidics/MEMS technology (microfluidic method [15–17]) and the method based on effervescence of dissolved gas due to depressurization at a decompression nozzle (a pressurized dissolution method [18,19]). Although bubble breakup methods can generate micro-bubbles at a high void fraction, the diameter of generated bubbles ranges widely and is larger than the other methods. The number densities of micro-bubbles generated by ultrasonic methods and microfluidic methods are not high whereas they can generate mono-dispersed fine micro-bubbles. The pressurized dissolution methods can generate fine micro-bubbles with a high bubble number density which is preferable in many industrial applications of micro-bubbles, though they require relatively higher energy consumption to generate micro-bubbles than the other methods.

We therefore focused on the pressurized dissolution method and examined influence of liquid velocity at the decompression nozzle throat on diameter and number density of micro-bubbles to understand the mechanism of a micro-bubble generation [20]. As a result, it was found that micro-bubbles are generated when

* Corresponding author.
E-mail address: hosokawa@mech.kobe-u.ac.jp (S. Hosokawa).

http://dx.doi.org/10.1016/j.expthermflusci.2014.09.010
0894-1777/

Nomenclature

A_{MV}	cross-section of PDA measurement volume (m^2)
C	concentration of dissolved air (kg/m^3)
C_s	saturation concentration of dissolved air at atmospheric pressure (kg/m^3)
DO	concentration of dissolved oxygen (kg/m^3)
d_{32}	Sauter mean diameter (m)
d_{Bi}	individual bubble diameter (m)
H	water level in dissolution tank (m)
J_L	liquid volumetric flux at nozzle throat (m/s)
N	sample number of bubbles (–)
N_B	data acquisition rate in PDA measurement (Hz)
n_B	bubble number density (m^{-3})
P	probability density function (–)
Q_L	liquid flow rate (m^3/s)
S	cross-section area of nozzle throat (m^2)
V	liquid velocity (m/s)
x^*_{GD}	mass fraction of a gasifiable dissolved gas (–)

Greek letters

α_B	bubble volume fraction (–)
θ_B	mean volume of single bubble (m^3)
ρ	liquid density (kg/m^3)

cavitation takes place in the decompression nozzle and the cavitation plays an important role in the micro-bubble generation. Since the dissolved gas concentration at the nozzle inlet is also an important parameter of micro-bubble generation, its influence on the diameter and number density of generated micro-bubbles has to be examined to understand the generation mechanism. In the present study, we therefore measure the diameter and number density of micro-bubbles at the downstream region of the nozzle by using phase Doppler anemometry (PDA) for several dissolved gas concentrations. Flow patterns in the nozzle are also observed by using a high-speed video camera. Generation mechanism of micro-bubbles is discussed based on dependences of the mean diameter and number density on the liquid velocity and the dissolved gas concentration.

2. Experimental apparatus

Fig. 1 shows a schematic of the experimental apparatus which is the same as the one in Hosokawa et al. [19] and Maeda et al. [20]. Water and air were used for the liquid and gas phases. Water was stored in the lower tank and supplied by the pump to the dissolution tank. Air was supplied by the compressor and mixed with water in the dissolution tank shown in Fig. 2, in which the air dissolved into the water through the air–water interface. Since the mass transfer rate between air and water increases with the gas–liquid interfacial area, the concentration of the dissolved air was controlled by changing the height H of the falling film (see Appendix A). The excess air, which did not dissolve into water, was exhausted from the top of the dissolution tank through the exhaust valve. The water with dissolved air flowed into the decompression nozzle shown in Fig. 3, the gap size, length and width of which were 1.0, 4.0 and 32.0 mm, respectively. Micro-bubbles were generated by decompression at the nozzle. Then, the water with micro-bubbles flowed into the vertical rectangular duct, the cross-section of which was 4×32 mm^2. Photographs of generated micro-bubbles are shown in Fig. 4. The water is opaque due to the presence of a lot of fine micro-bubbles, whereas it is clean near the bottom of the beaker due to decrease in micro-bubble density caused by buoyancy. The water flowed into the lower tank through the upper tank. The micro-bubbles were released from the water to the atmosphere through the water surface in the upper and lower tanks, and no bubbles presented at the inlet of the decompression nozzle. The water temperature was kept at 298 ± 0.5 K.

Experimental ranges of the liquid volumetric flux J_L at the nozzle throat and the mass fraction x^*_{GD} of gasifiable dissolved gas at the nozzle inlet were $J_L = 10$–14 m/s and $x^*_{GD} = 0.0$–1.69×10^{-5}, respectively. They are defined by

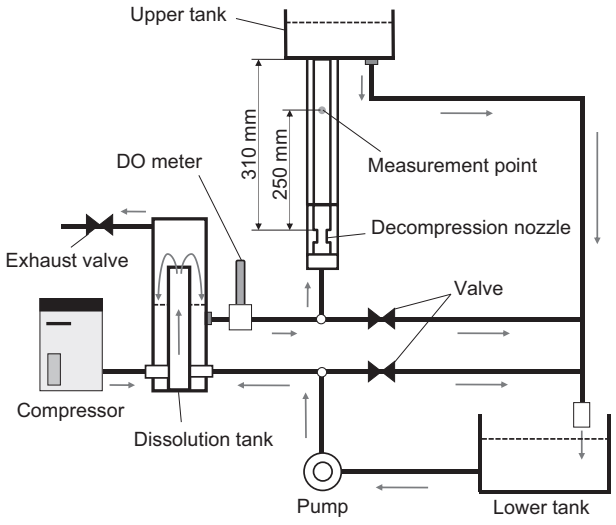

Fig. 1. Schematic of experimental apparatus.

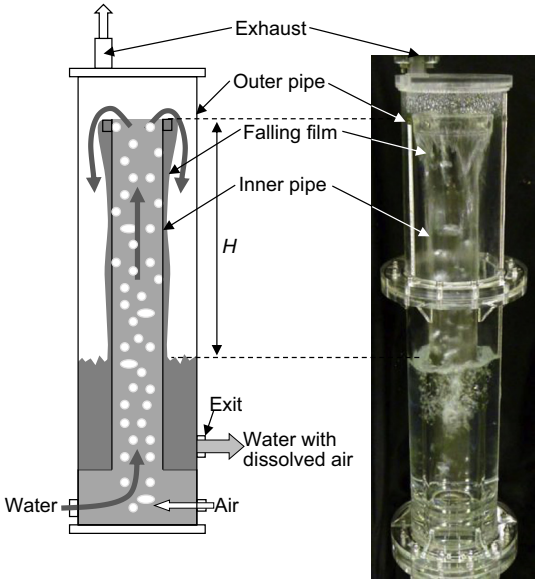

Fig. 2. Dissolution tank.